Eksploatacja i Niezawodnosc – Maintenance and Reliability
Volume 22 (2020), Issue 4
journal homepage: http://www.ein.org.pl

Article citation info:
Blaut J, Breńkacz Ł. Application of the Teager-Kaiser energy operator in diagnostics of a hydrodynamic bearing. Eksploatacja i Niezawodnosc – Maintenance and Reliability 2020; 22 (4): 757–765, http://dx.doi.org/10.17531/ein.2020.4.20.

Application of the Teager-Kaiser energy operator in diagnostics of a hydrodynamic bearing

Indexed by:
Web of Science Group

Jędrzej Blaut [a], Łukasz Breńkacz [b]*

[a] AGH University of Science And Technology, al. Mickiewicza 30, 30-059 Kraków, Poland
[b] Department of Turbine Dynamics and Diagnostics, Institute of Fluid Flow Machinery, Polish Academy of Sciences, Fiszera 14, 80-231 Gdańsk, Poland

Highlights

- Use of the Teager-Kaiser energy operator to evaluate the state of unbalance.
- Tests of the rotor supported on hydrodynamic plain bearings were conducted.
- A diagnostic parameter was used to assess the technical condition of the machine.

Abstract

The paper presents the use of the Teager-Kaiser energy operator (TKEO) to evaluate the state of rotor unbalance. The method was developed in 1990 by Kaiser and involves a simple calculation of signal energy. It has been used before in diagnostics, e.g. during the evaluation of instability of hydrodynamic bearings and as a diagnostic symptom of gearbox damage. This paper is the first to present the use of the Teager-Kaiser method to evaluate the rotor unbalance in hydrodynamic bearings.

Keywords

Teager-Kaiser energy operator, rotor unbalance, hydrodynamic bearings, rotor dynamics.

1. Introduction

The search for new methods to evaluate the condition of machines in technical diagnostics is related to extension of the expected time of reliable operation. There are hardware solutions for better measurements, and signal processing methods that allow a quicker and more reliable decision making by experts. The nonlinear analysis of acoustic signals has become popular in recent years. Based on the observation of operating parameters of equipment, it is possible to draw conclusions about the origin of the condition and also to predict the future condition of the machine. The main postulate of technical diagnostics connects the increase of vibroacoustic energy with the growing wear of machines during their use. It leads to the need to look for new, better diagnostic methods for better determination of the border between the correct operation and the moment after which further operation involves a risk of failure. The operation of plain bearings is strongly nonlinear under some conditions, the phenomena accompanying the wear are impossible to be linearized [10]. Methods are developed for linearization of non-stationary signals describing the properties of mechanical systems [7], also combining the resampling and order spectrum [21]. The use of the Teager-Kaiser energy operator is one of the new and promising methods of vibroacoustic diagnostics [5, 11]. The paper presents the experimental studies of the impact of rotor unbalance on the value of energy operator.

The unbalance of rotating machines is very important for a number of reasons. It is most often noticed when e.g. a steering wheel in a car vibrates at some speeds or when the brake pedal vibrates under the foot; generally, we deal with unbalance every day. It can be said that the unbalance occurs when the distribution of the rotor weight is uneven; to a greater or lesser degree, this phenomenon applies to each rotating machine. Unbalance creates centrifugal forces, vibration and noise during the rotation. Bearings, housings and foundations can be exposed to loads caused by vibration resulting from unbalance, causing increased wear. The products with unbalanced parts often have a shorter life. Vibration can decrease the bolted and clamp connections until the parts come loose. Vibration also destroys electric switches, and the conductors and cables can crack at the joints. Unbalance can also significantly reduce the operational safety of a machine. Vibration caused by the unbalance and disturbing the machine operation is reduced by the balancing. It involves the even distribution of the rotor weight to reduce the centrifugal forces acting on the bearings. Precise use of power tools is more difficult when they are not balanced well. It also affects the user comfort, as it can shorten the time to perform the work. In case of CNC (Computerized Numerical Control) machining centres, absence of unbalance control leads to the impossibility to maintain the production repeatability and the reduced quality. An important aspect in the evaluation of technical condition is the evalu-

(*) Corresponding author.
E-mail addresses: J. Blaut - blaut@agh.edu.pl, Ł. Breńkacz - lukasz.brenkacz@imp.gda.pl

ation in real time, which can increase the reliability. An example of such evaluation for a cutting tool was presented e.g. by Kozłowski et al. in [20]. The noise and vibration during the equipment operation are among the criteria considered by potential buyers. Excessive emission of acoustic waves or arduous vibration have a negative impact on product competitiveness, making it difficult to achieve market success.

Czmochowski et al. [9] presented the studies of excessive vibration in rotating machines in steady and transient states, using large-diameter axial fans as an example. The vibration is caused by unbalance, misalignment, bearing failure, etc. The authors emphasized that the transient state occurs frequently. It appears mostly during the start-up and is caused by "passing" through critical speeds which induce the object vibration. The main parameters affecting the vibration level were identified.

Kosmol [19] showed an analysis of a rolling bearing, considering various parameters affecting the contact forces. The bearing ring speed, the preliminary strain of the bearing and the fit in the bearing significantly affect the resistance to motion and as a result the bearing operation. Churdzik and Warda [8] presented the fatigue life prediction of a bearing subjected to a combined load. Geometrical parameters of the bearing, including radial clearance and shape of rolling elements, were included in the calculations. The calculation results showed that the axial load of a radial bearing and the inclination of rollers reduce the fatigue life. Knotek et al. [18] presented the impact of turbocharger disc unbalance. A structural rotor model and a hydrodynamic model of a bearing with a floating ring were built as an assumption in the "multibody dynamics" type of software. The errors in disc manufacture and parallelism errors cause an increased unbalance. Zhao et al. [29] described a method to improve the vibration response by multioptimization of unbalance distribution and rotor axis bending. The basic step was a quantitative reconstruction of the bending and installation angles. The rigid rotor balancing method was used, meaning that the small balanced reaction forces were considered better results. The dynamic model based on elliptical bearings was analysed using the FEM (Finite element method).

Shamsah and Sinha [16] showed the unbalance calculation with a reduced number of sensors. The authors emphasize that the unbalance must be regularly checked in order to ensure the correct operation of a machine. The most popular practice is to measure the vibration in two perpendicular directions along with the tachometer signals. The authors stress that many people believe that measuring the vibration in vertical and horizontal direction reflects the machine dynamics better. In the paper, instead of two sensors placed perpendicularly, they used one sensor at the angle of 45 degrees. One sensor partially recorded signals from the vertical and horizontal direction.

Plantegent et al. [22] presented the experimental analysis of the thermal unbalance of a flexible rotor. The Morton effect is related to the thermal increase of the amplitude of the rotor synchronic speed. The rotor bending is related to the increased unbalance. The tests of increasing and decreasing the rotational speed show the amplitude and phase hysteresis loops of synchronic vibration. The tests for constant rotational speeds show the changes of amplitude and phase. The obtained results are explained as an uneven distribution of the rotor temperature.

Zou et al. [30] used the augmented Kalman filter to identify unbalance. Theoretical analyses and experimental studies were performed. This method can be used to calculate the unbalance in real time and is unaffected by measuring and modelling errors, making the determination of unbalance more accurate. Wand et al. [27] showed a method for simultaneous identification of unbalance and dynamic coefficients of rolling bearings using the uniform continuous Raleigh beam as a model. Amroune et al. [2] showed an algorithm allowing the number of adding correctional eights to be reduced.

One of the most popular methods for the evaluation of unbalance is standards, e.g. ISO 1940 [31] which defines a rigid rotor as a rotor whose unbalance can be corrected in any two planes. After balancing, the residual unbalance does not change significantly for all speeds until the rated speed. The rigid rotor is equated with a rigid mass. As a result of rotor rotation at angular speed ω, acts the centrifugal force on radius r on the unbalanced mass m_u:

$$F = m_u \cdot r \cdot \omega^2. \tag{1}$$

The static moment of this mass relative to the rotor axis is called unbalance:

$$N = m_u \cdot r. \tag{2}$$

The unbalance is a vector quantity with direction and sense defined by the vector of the unbalanced centrifugal force F. Value m_u is usually given in grams, and radius r in millimetres, so the unbalance is given in [g·mm]. Balancing is a process to correct the rotor mass, involving adding or subtracting on the correction radius such correctional mass for which the sum of centrifugal forces, and hence the sum of unbalance, is zero.

If the rotor axis and its central main inertia axis are parallel, such unbalance is called static unbalance. Such unbalance occurred during the laboratory tests presented in this paper. If a rotor has only static unbalance, it can be balanced in any plane passing through the centre of gravity by placing a correctional unbalance in this plane. If the rotor axis and its central main inertia axis intersect in the centre of gravity, such unbalance is called moment unbalance. The third possible condition is dynamic unbalance which is the most general state of unbalance in which the rotor rotation axis and its inertia axis are not parallel (are skew). This unbalance state is unequivocally determined by the unbalance vector and the main unbalance moment or by two unbalance vectors lying on any transversal planes. The dynamic unbalance can be considered as a superposition of the static unbalance and the moment unbalance, where the planes of these two unbalances do not coincide.

The effect of unbalance vector orientation on the oil whirls in created rotors was shown by AL-Shudeifat et al. in [1]. The authors conducted theoretical and experimental studies. It was determined that the change of the unbalance force vector significantly affects the amplitude peak values. As a result, the critical speeds of a cracked rotor are shifted towards higher or lower values, depending on the unbalance force vector orientation. One of the most important findings is that there is a specific value of the unbalance force angle for which critical vibration is almost eliminated in a cracked rotor compared with an uncracked rotor. Spagnol and Xiao [26] showed an analysis of mechanic response of an unbalanced cracked rotor taking into account the "breathing mechanism". Unlike in other studies, the authors assumed that the source of fatigue cracking is not related to the weight, but they analysed the impact of dynamic forces related to the unbalance.

Flexible rotors can be balanced with the use of ISO 5343 [32]. The balancing of a flexible rotor in two correction planes does not provide the same degree of unbalance for all speeds up to the maximum operating speed due to the flexural strains. The effect of unbalance on a flexible rotor supported on floating ring bearings was presented by Singh and Gupta [25]. As the rotor speed increases, the forces caused by unbalance are more important than the forces coming from the motor.

The unbalance is usually corrected by adding a balancing mass. Heindel et al. published a paper in which they showed that the unbalance elimination is possible by using active bearings [12, 13]. The authors proved theoretically and practically that active bearings are able to eliminate both the bearing vibration and the rotor resonance. The active bearings can displace the rotor so that its centre of mass always remains in the centre of rotation (on the line of rotation). The proposed controller is able to maintain such a state at any rotational

speed, leading to reduced bearing vibration and elimination of resonance. The authors analytically showed that a closed-loop system is always stable, even without knowing all rotor properties. The generalization of the proposed approach allows it to be applied for all types of active bearings.

An accurate mathematical description of automatic rotor balancing can be found in [4, 23]. The model uses a differential equation which includes the matrices of masses, damping and rigidity. It can be used to model the disc inertia, shaft bending and linear-viscotic external friction resistance.

The laboratory stand for testing of small rotors was built in order to analyse a rotor-bearings system and study the defects such as bearing failure, rotor unbalance, misalignment, etc. The stand is shown in Fig. 1. Its weight without the support structure is about 60 kg.

Fig. 1. Laboratory test stand

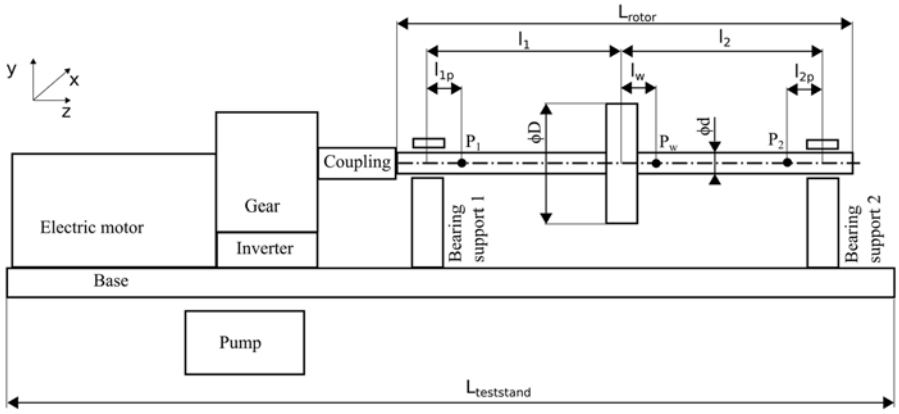

Fig. 2. Laboratory stand diagram

Fig. 2 presents the diagram of the laboratory stand with dimensions and the most important components. The stand length is 125 cm, width 36 cm, and height 65 cm. The figure also shows the system of coordinates used during the experiments. The laboratory stand base is a 13-mm thick steel plate. Attached to it are two channel bars which allow the height adjustment and levelling. The rotor was fixed in two bearings. The system was driven by a 3-phase motor of maximum speed 3,450 rpm controlled by a 1.5 kW inverter. The motor was connected to a gearbox which increased the rotational speed about 3.5 times. The drive system allowed reaching the speed up to 12,000 rpm. The coupling diameter was 50 mm and length 60 mm. The bearings were fed by a pump generating maximum pressure of 35 PSI (0.24 MPa). The oil pressure during the experiments was 23 PSI (0.16 MPa).

The length of the tested rotor was L_{rotor} = 920 mm. The distance between the coupling and the first support was 170 mm. The rotor was placed in two bearing supports. The distance between supports (i.e. $l_1 + l_2$) was 580 mm. The bearing closer to the motor is marked as 1, the bearing on the other side of the rotor is marked as 2. The rotor disc was placed midway between the supports, so lengths l_1 and l_2 are equal (Fig. 2). The rotor diameter was 19.02 mm (about ¾″), and the rotor disc diameter was 152.4 mm (6″). Uniaxial displacement sensors were placed in bearing supports. The eddy current sensors were placed in points P_1 and P_2, located at equal distances ($l_{1p} = l_{2p}$ = 25 mm) from bearing centres. The sensors measuring the displacement in axis X were placed 20 mm away from bearing centres, while the sensors measuring the displacement in axis Y were placed 30 mm away from bearing centres. Such a shift is necessary because the eddy current sensors cannot operate in the same plane. The eddy current sensors were placed at the 90 degrees angle relative to each other (and 45 degrees relative to the global system of reference). To provide safety, the rotor-bearings system was equipped with a closable guard made of transparent plastic.

The rotor was supported on two hydrodynamic bearings of identical geometrical parameters. The lubrication gap in relation to the shaft radius was 76 μm. The bearing photograph and its schematic are shown in Fig. 3. The bearing length was L = 12.6 mm. The oil to the bearings was fed through two holes placed on the left-hand and the right-hand of the shaft. The diameter of the holes was 0.1″ (2.54 mm). The oil viscosity class was ISO 13.

Two triaxial accelerometers were placed on the bearing supports. Fig. 4 presents a cascade chart illustrating the rotor's increasing speed from 900 to 10,000 rpm recorded by the accelerometer placed on the second bearing support (farther from the coupling). The acceleration signal was divided into parts, and the Fast Fourier Transform (FFT) was performed for each part. The horizontal axis presents the frequency values from the FFT. The lower part of the chart includes the FFT results for low rotational speeds, and the values for high rotational speeds are shown in the upper part. The line connecting the amplitude peaks, which starts from the left bottom corner, shows the frequencies related to the rotational speeds (1X, 2X and 3X). From the diagnostic point of view, important are the vibration frequencies which are related to the rotational speed (1X) and its relation to the sub-synchronous vibration (e.g. 1/2X) and super-synchronous vibration (e.g. 2X, 3X). The chart indicates that the values of synchronous vibration (1X) are dominant relative to the sub-synchronous values (1/2X) which means that no clear oil vortexes or friction of the rotor against the bearing sleeve was observed in the hydrodynamic bearings. The component 2X is increased in the system, which may be related to e.g. the displacement of the axis of the two rotors (these symptoms may be connected also with other causes, e.g. the rotor bending).

2. Teager-Kaiser energy operator

The energy operator in continuous form is defined as [17]:

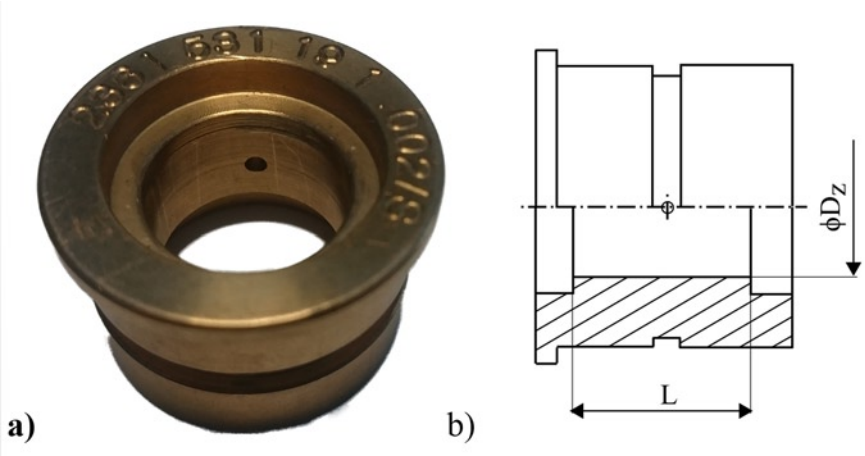

Fig. 3. a) Hydrodynamic bearing, b) Bearing schematic

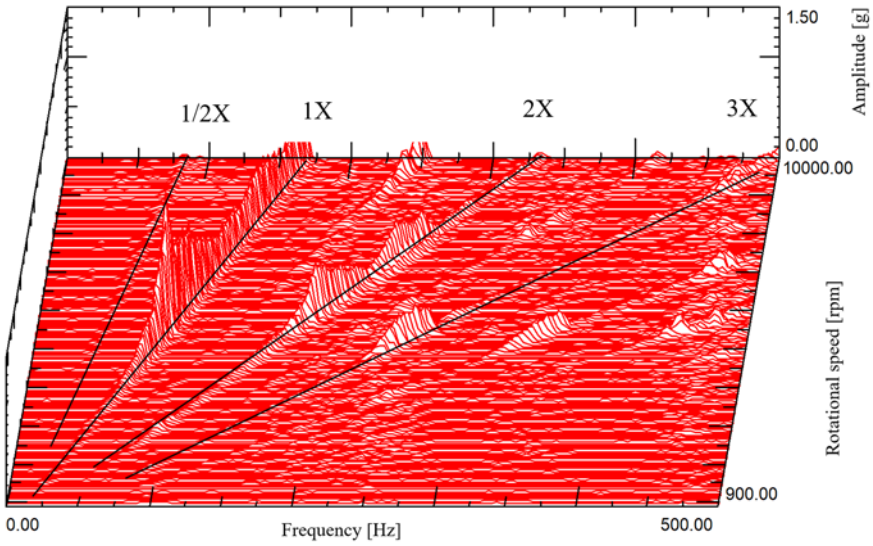

Fig. 4. Cascade chart presenting the acceleration on the second support in direction X

$$\Psi(x(t)) = \dot{x}^{2}(t) - x(t)\,\ddot{x}\,(t), \tag{3}$$

where:

x(t) – displacement,

$\dot{x}(t)$ – first time derivative of displacement,

$\ddot{x}(t)$ – second time derivative of displacement.

Originally, this method was used for speech analysis [17]. It was successfully applied for the analysis of gearbox operation by Gałęzia et al [11]. Antoniadou et al. [3] used the energy operator for condition monitoring of a wind turbine gearbox under varying load conditions. Henríquez et al. [14] showed that the energy operator [6] can be used also in analysis of a helicopter bearing. Blaut et al. [5] showed the possibility of using the Teager-Kaiser energy operator as an estimator of hydrodynamic stability of a plain bearing, indicating an instantaneous 50% increase of TKEO amplitude in case of hydrodynamic instability in a small time window based on the signal of bearing journal displacement relative to the bearing sleeve. The authors showed that the TKEO amplitude is related to the energy changes in the system.

The thesis tested in this paper was as follows: by determining the value of TKEO amplitude based on the movement of a plain bearing journal one can infer the changes of the operating parameters of the rotor-bearing system such as operation stability and unbalance. The thesis was tested experimentally. The plain bearing operation before and after the balancing was observed during the experiments.

3. Description and results of experimental tests

Within the experiments, the Teager-Kaiser energy operator was used to detect unbalance of a rotor supported in two hydrodynamic bearings. The analyses were conducted based on the recorded displacement signal of the bearing journal relative to its sleeve. The signals were recorded using the LMS Scadas Mobile data acquisition module and then analysed as discussed below. The measurements were made with the frequency of 25,600 samples per second.

3.1. Displacement

Fig. 5 presents the displacements recorded by the eddy current sensors for two cases of rotor unbalance. In the experiments with the unbalance described in the charts as “unb”, the unbalance was twice as greater as allowed by ISO 1940-1 in class G6.3 [31]. In the experiments in the other case of unbalance described as “bal”, the rotor was balanced in class G6.3. The left-hand chart shows the displacement of bearing journals and the right-hand one the displacements for the middle part of the rotor. By comparing the bearing vibration amplitudes, it can be seen that the vibration amplitude is greater on the first bearing before resonance, while after passing through the resonance (above 6,000 rpm) the vibration amplitude is greater for the second bearing. This happens for both, the unbalanced and balanced bearing. The probable cause is the change of the main ellipse axis after passing through the resonance.

The greatest displacement amplitudes were observed near the test stand resonance (about 5,000 – 6,000 rpm). This is typical for any rotating machine which is supercritical, meaning that the nominal rotational speed is higher than the resonance speed. In two measurements, there was an unexpected decrease in the ratio of the displacement amplitude before the balancing to the displacement amplitude after the balancing. It was recorded at 1,000 rpm for bearing 1 in the x-direction (0.4% decrease) and bearing 2 in the y-direction (5% decrease). The greatest increase in the ratio of the displacement amplitude before the balancing to the displacement amplitude after the balancing occurred at 5,000 rpm for bearing 2 in the y-direction (70% increase).

3.2. Vibration acceleration

The recorded acceleration allowed the comparison of the system instability detection effectiveness using the TKEO in relation to the expected increase of the vibration acceleration. Fig. 6 presents the vibration acceleration recorded by the accelerometers placed on bearing supports. The tests were made for two cases of rotor unbalance, as in the case of displacements described above. Part a) of the figure presents the vibration acceleration of bearing supports in the horizontal direction, and part b) in the direction of gravity (Y).

The vibration acceleration amplitude obtained after the balancing was reduced in 23 of 32 measurements. The acceleration amplitude was reduced most often (at 1,000, 2,000, 3,000 and 4,000 rpm) in the direction of X-axis for bearing No. 1, and in single cases for other

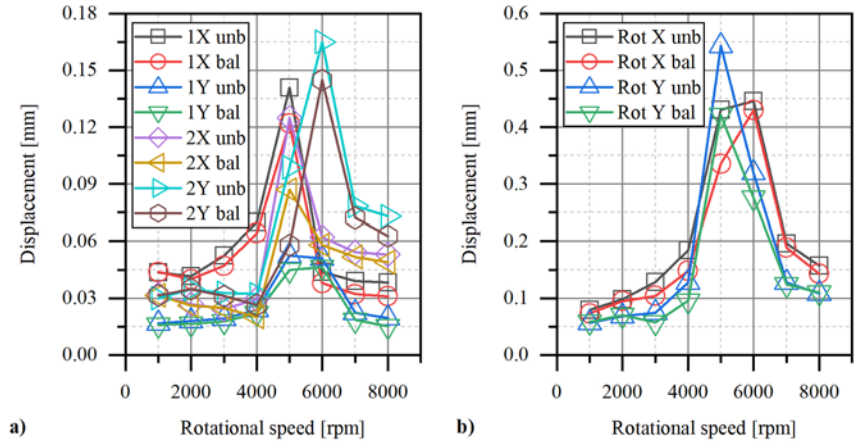

Fig. 5. Displacement depending on the rotational speed for the unbalanced and balanced rotor. a) displacement of bearing journals, b) displacement of rotor disc

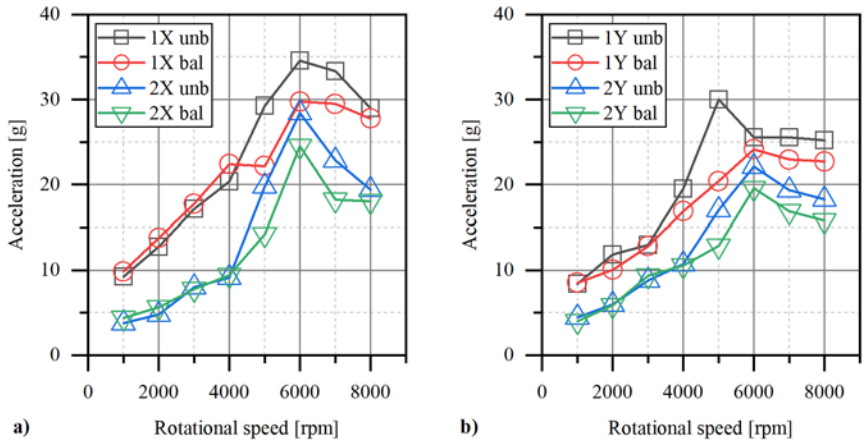

Fig. 6. Acceleration of bearing supports depending on the rotational speeds: a) displacement of bearing journals, b) displacement of rotor disc

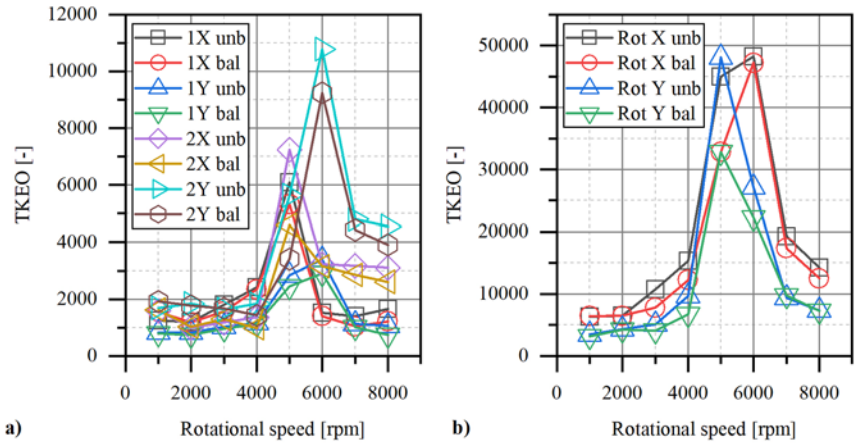

Fig. 7. Values of the energy operator (TKEO) depending on the rotational speed for unbalanced and balanced rotor a) TKEO for bearing journals, b) TKEO for rotor disc

measurement locations. The greatest acceleration amplitude decrease was at speeds above 4,000 rpm. The greatest acceleration amplitude increase before and after the balancing was at 5,000 rpm for bearing 1 in the y-direction (47% increase).

3.3. TKEO

Fig. 7 presents the TKEO values calculated based on the displacement signal using the formula (3). The tests were made for two cases of rotor unbalance. Part a) of the figure shows the TKEO value for the bearing journal, and part b) for the middle part of the rotor. Comparing the TKEO values with the displacement and acceleration amplitude, one can notice an analogy of maximums reached for signals from axes x and y. For the displacement, acceleration and TKEO, the maximum is at 5,000 rpm in the x-axis and at 6,000 rpm in the y-axis. The TKEO value obtained after the balancing of the system was reduced in 26 of 32 measurements. The ratio between the values before and after the balancing was maximally 70% for the displacement signal, 47% for acceleration, and 65% for TKEO.

The force generated by unbalance increases according to formula (1). The analysis of the amplitude-frequency spectrum of the system indicates that the unbalance is related to the increase of the frequency range which depends on the rotational speed. The examples of amplitude-frequency spectra for 33 speeds are presented in the "Discussion" section. The unbalance is related to the increase of the system absolute vibration, which was presented in section 3.2 ("Vibration acceleration"). The TKEO value is also related to the acceleration. The TKEO values before and after the balancing differ by $-20 \div +65\%$. The values of displacement, acceleration and TKEO in some cases are lower before the balancing that after the balancing, particularly for low speeds, which means that after the balancing the vibration was reduced for the lowest speeds and increased for the remaining speeds. Tables 1 and 2 present the ratio of TKEO values obtained before and after the rotor balancing in comparison with the analogous acceleration values (Table 1) and displacement values (Table 2). The determined ratio of the TKEO and acceleration values for measurement points (Table 1) indicates that these values are sometimes greater and sometimes lesser than each other. The displacement signal (Table 2) is more related to the balancing process. The ratio between values before and after the balancing is less than one only for two measurement points. This means that the displacement amplitude decrease was noted after the balancing in two measuring points. For comparison, the analogous value for acceleration is 9, and 6 for TKEO. The determined ratio of the TKEO values and the displacement values (Table 2) indicates that these values are sometimes greater and sometimes lesser than each other. However, the observed TKEO value is never less than one when the displacement value is less than one.

Table 1. Comparison of TKEO values and acceleration values (Acc) before and after the balancing for axes x and y (for bearings 1 and 2)

rpm	1x unbalanced/ balanced		2x unbalanced/ balanced		1y unbalanced/ balanced		2y unbalanced/ balanced	
	TKEO	Acc	TKEO	Acc	TKEO	Acc	TKEO	Acc
1,000	0.80	0.94	0.97	0.86	1.05	0.98	0.88	1.13
2,000	1.017	0.93	0.97	0.86	1.12	1.18	1.04	1.02
3,000	1.17	0.97	0.90	1.03	1.06	1.01	0.98	0.94
4,000	1.03	0.91	1.40	0.97	1.02	1.16	1.29	1.02
5,000	1.14	1.32	1.57	1.39	1.16	1.47	1.65	1.33
6,000	1.09	1.16	1.02	1.16	1.17	1.06	1.17	1.13
7,000	1.34	1.13	1.11	1.25	1.12	1.11	1.08	1.15
8,000	1.36	1.05	1.19	1.07	1.42	1.11	1.16	1.16

Table 2. Comparison of TKEO values and displacement values (Disp) before and after the balancing for axes x and y (for bearings 1 and 2)

rpm	1x unbalanced/ balanced		2x unbalanced/ balanced		1y unbalanced/ balanced		2y unbalanced/ balanced	
	TKEO	Disp	TKEO	Disp	TKEO	Disp	TKEO	Disp
1,000	0.80	1.00	0.97	1.02	1.05	1.06	0.88	0.95
2,000	1.017	1.04	0.97	1.02	1.12	1.10	1.04	1.00
3,000	1.17	1.12	0.90	0.98	1.06	1.09	0.98	1.05
4,000	1.03	1.09	1.40	1.48	1.02	1.08	1.29	1.21
5,000	1.14	1.16	1.57	1.44	1.16	1.17	1.65	1.71
6,000	1.09	1.15	1.02	1.07	1.17	1.09	1.17	1.14
7,000	1.34	1.22	1.11	1.05	1.12	1.19	1.08	1.09
8,000	1.36	1.24	1.19	1.08	1.42	1.28	1.16	1.16

4. Discussion

The paper presents the application of TKEO in the monitoring of the system unbalance. It was noticed that the TKEO values increased by several dozen percent for the system before the balancing process. The increase is conditional on the simultaneous increase of the vibration amplitude. For low speeds, the vibration in the system was less after the balancing process.

The impact of the bearing vibration trajectory on the TKEO was analysed. According to the literature, the TKEO is sensitive to trajectory changes [24] – the occurrence of oil vortexes causes a significant increase in the TKEO. The trajectories of the shaft vibration relative to the bearing sleeve changed during the experiment. However, a similarity was noticed between the trajectory shapes for different rotational speeds before and after the rotor balancing. The authors focused on the comparison of the rotor operation with two different unbalances. Because during the hydrodynamic bearing operation it is impossible to change only one parameter – the unbalance, also other changes in the system were observed. The flattened eight-shaped trajectory is related to the increased 2X component in the spectrum. Such symptoms suggest that at higher rotational speeds, the bearing overload occurs (increased centrifugal force caused by unbalance).

In case of low rotational speeds, no significant differences between the displacement and acceleration amplitude were noted. This phenomenon is clearly visible on amplitude-frequency spectra obtained for successive speeds. Fig. 9 presents successive speeds with a visible increase of the speed-related component and proportionally lower disturbance. For low speeds, the component frequencies of vibration acceleration are not directly related to the rotational speed and make a wide frequency range above 150 Hz. In the analysed case, the rotor vibration above 150 Hz may have been caused by the test stand vibration, e.g. the pump feeding the bearing. The vibration caused by the system unbalance is particularly important at high rotational speeds when significant system energy changes take place.

During the experiment, in order to verify the relationship between the stable bearing operation and the TKEO value, analysed was the shape of trajectories (orbit plot) obtained before and after the balancing. The shape of trajectories conforms to our expectations; the bearing operation after the balancing is more stable – the trajectory resembles an ellipse, but before the balancing, the shaft in the bearing sleeve moves in the shape resembling eight. The TKEO values for the discussed signals are (see

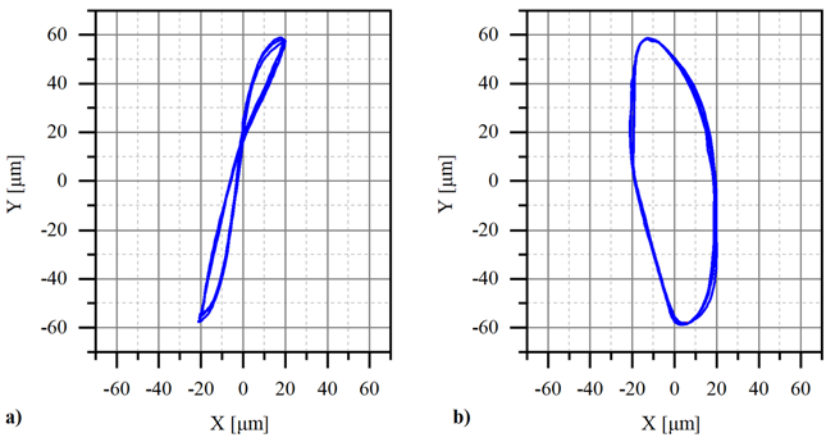

Fig. 8. a) Unstable trajectory for unbalanced rotor at 5,000 rpm. b) Stable trajectory for balanced rotor at 5,000 rpm

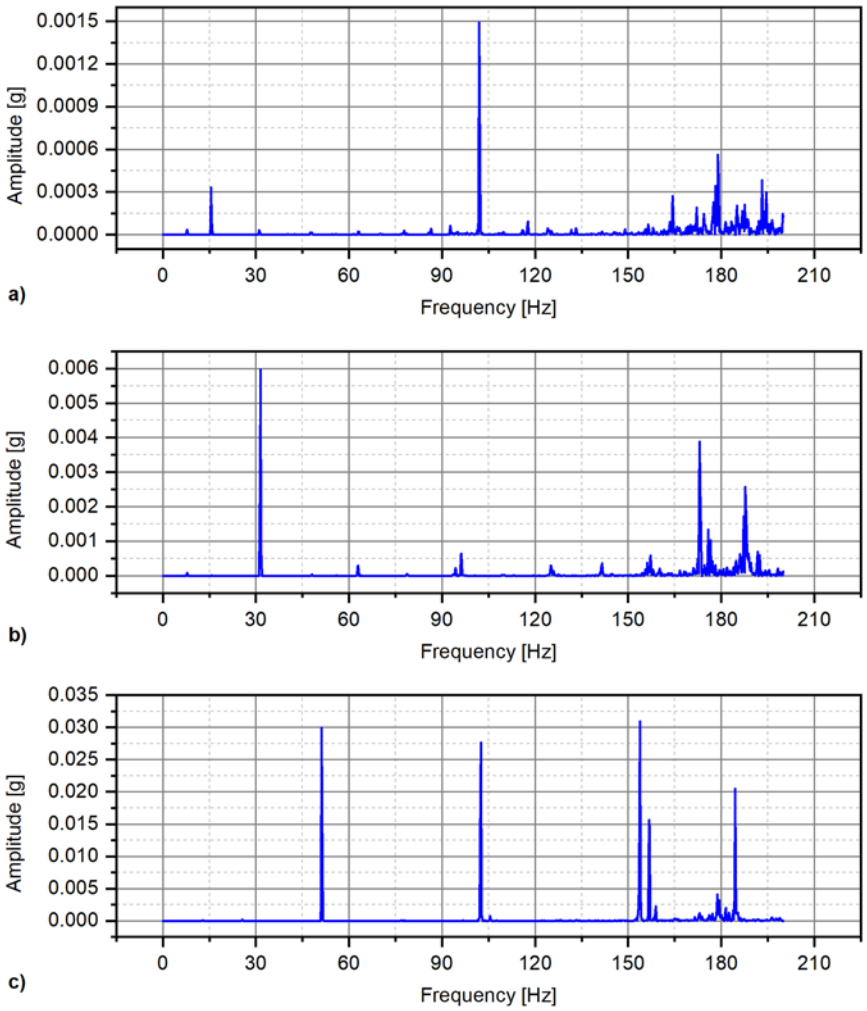

Fig. 9. Amplitude-frequency spectrum for acceleration signal 1x unbalance at rotational frequency: a) 17 Hz, b) 31 Hz, c) 51 Hz

Table 1): 1x unbalanced/ balanced: 1.14, 1y unbalanced/ balanced 1.16. Despite a significant change of trajectory shape, the TKEO increase is not that significant as for the displacement signal from bearing 2: 2x unbalanced/ balanced 1.57, 2y unbalanced/ balanced 1.65.

The paper also presents the percentage ratio of the values before the balancing to the values after the balancing. For the displacement signal, it was maximally 70%, 65% for the TKEO, and 47% for acceleration. These values may be significant when the method is implemented in the systems troubled by disturbance (electrical or mechanical). At the laboratory test stage, this problem is not obvious and the paper aims at popularizing the method, particularly in industrial applications. An additional advantage of using the TKEO is that the signal does not need to be filtered which may be required when the displacement or acceleration signal is noised.

The analysis indicates a relationship between the shape of vibration trajectory and the TKEO value. The more the trajectory shape differs from circular, the more component frequencies occur in the signal. The relationship is described for a simple mechanical system with one degree of freedom $x = Acos(\omega t)$, and substituting it into equation (3) we obtain:

$$\Psi(x(t)) = (-A\omega\sin(\omega t))^2 - A\cos(\omega t)(-\omega 2A\cos(\omega t)) = A^2\omega^2(\sin^2(\omega t) + \cos^2(\omega t)) = A^2\omega^2 \qquad (4)$$

The TKEO value depends both on the signal amplitude and frequency, which was proved during experiments on the test stand for various rotational speeds.

5. Summary and conclusions

As technology progresses, we observe the development of diagnostic methods. The analysis of an increased number of diagnostic parameters allows making more conscious decisions concerning the technical condition of a machine. In the advanced diagnostic systems, there is a tendency to increase the number of various measuring sensors, but also to develop software for interpretation of results. The determination of trends, as well as warning and alarm values, becomes a standard. Usually, such operations are preformed directly on the measured signal, that is most often on the values of displacement, speed or acceleration. Within this project, we proposed a new approach: the application of the Teager-Kaiser energy operator to evaluate the rotor unbalance. For this purpose, the experimental tests were conducted for two cases of rotor unbalance.

In order to evaluate the technical condition of any technical object, it is necessary to present its basic operating parameters, as shown at the beginning of the paper. The tested object was a laboratory stand for the analysis of the dynamics of a rotor supported on hydrodynamic bearings. The bearing journals diameter was 19.02 mm. Between the bearings was a disc with holes in which the unbalance was controlled. It was also a plane in which the rotor was balanced. The photograph of the stand and its diagram are shown in the paper. As a result of this arrangement of the laboratory stand, it was possible to make calculations using the energy operator for unbalance on two different levels. The cascade charts were plotted from which it is possible to determine the dynamic rotor behaviour (the FFT results) over the entire range of rotational speeds, from 900 to 10,000 rpm. The hydrodynamic bearings which supported the rotor were described as well.

The results of the analyses were presented for two cases of unbalance, comparing not only the values of the energy operator but also the measured rotor displacement and acceleration of bearings. The plotted vibration trajectories very clearly indicate the differences between the balanced and unbalanced systems. The differences in the operation of balanced and unbalanced systems are visible for all analysed signals (displacement, acceleration and TKEO), proving that all of them can be used successfully to evaluate the unbalance. The unbalance analyses carried out by means of the energy operator within this project were based on the unbalance changes directly made in the system. Zhang and Zhang [28] presented the method for calculation of the reliability of parallel systems in case of coexisting failures caused by a common cause and load-sharing failures. The authors calculated the average fitness time of the tested system in various configurations. The TKEO can also be used for similar analyses. The method for finding correlations using inaccurate statistical data was presented, e.g. by Hryniewicz [15].

More and more papers have been published in recent years, showing the methods to use the energy operator developed in 1990 [17]. The results of studies are published presenting the energy operator usefulness in various branches of diagnostics. One of the papers [24] shows that the energy operator can be used in the process of automatic rotor balancing. The authors of this paper hope that the comparison of results showing how the value of the energy operator changes with the results of classic diagnostic methods will contribute to the application of this potentially very useful diagnostic tool in evaluating technical condition of machines.

Acknowledgment

The project was financed by the Polish Ministry of Science and Higher Education [project No. 16.16.130.942].

References

1. Al-Shudeifat M A, Al Hosani H, Saeed A S, Balawi S. Effect of Unbalance Force Vector Orientation on the Whirl Response of Cracked Rotors. Journal of Vibration and Acoustics, Transactions of the ASME 2019; 141(2): 1-10, https://doi.org/10.1115/1.4041462.
2. Amroune S, Belaadi A, Menasri N et al. New approach for computer-aided static balancing of turbines rotors. Diagnostyka 2019; 20(4): 95-101, https://doi.org/10.29354/diag/114621.
3. Antoniadou I, Manson G, Staszewski W J et al. A time-frequency analysis approach for condition monitoring of a wind turbine gearbox under varying load conditions. Mechanical Systems and Signal Processing 2015; 64-65: 188-216, https://doi.org/10.1016/j.ymssp.2015.03.003.
4. Artyunin A I, Sumenkov O Y. Simulation of the Automatic Balancing Process of A Rotor, Rigidly Fixed in the Housing on Elastic Supports 2019; 188: 10-14, https://doi.org/10.2991/aviaent-19.2019.2.
5. Blaut J, Korbiel T, Batko W. Application of the Teager-Kaiser energy operator to detect instability of a plain bearing. Diagnostyka 2016; 17(4): 99-105.
6. Blaut J, Rumin R, Cieślik J et al. Application of TKEO in the process of automatic balancing of the rotor. AUTOBUSY - Technika, Eksploatacja, Systemy Transportowe 2019; 20(1-2): 161-166, https://doi.org/10.24136/atest.2019.028.
7. Burdzik R, Konieczny Ł, Warczek J, Cioch W. Adapted linear decimation procedures for TFR analysis of non-stationary vibration signals of vehicle suspensions. Mechanics Research Communications 2017; 82: 29-35, https://doi.org/10.1016/j.mechrescom.2016.11.002.
8. Chudzik A, Warda B. Fatigue life prediction of a radial cylindrical roller bearing subjected to a combined load using FEM. Eksploatacja i Niezawodnosc - Maintenance and Reliability 2020; 22(2): 212-220, https://doi.org/10.17531/ein.2020.2.4.
9. Czmochowski J, Moczko P, Odyjas P, Pietrusiak D. Tests of rotary machines vibrations in steady and unsteady states on the basis of large diameter centrifugal fans. Eksploatacja i Niezawodnosc - Maintenance and Reliability 2014; 16(2): 211-216.
10. Dąbrowski Z, Dziurd J. Increase of non-linear disturbances during machines operations. Journal of Machine Construction and Maintenance 2017; 1: 37-44.
11. Gałęzia A, Gumiński R, Jasiński M, Mączak J. Application of energy operators for detection of failures in gearboxes. Mechanics Research Communications 2017; 82: 3-8, https://doi.org/10.1016/j.mechrescom.2017.02.008.
12. Heindel S, Becker F, Rinderknecht S. Unbalance and resonance elimination with active bearings on a Jeffcott Rotor. Mechanical Systems and Signal Processing 2017; 85: 339-353, https://doi.org/10.1016/j.ymssp.2016.08.016.
13. Heindel S, Müller P C, Rinderknecht S. Unbalance and resonance elimination with active bearings on general rotors. Journal of Sound and Vibration 2018; 431: 422-440, https://doi.org/10.1016/j.jsv.2017.07.048.
14. Henríquez Rodríguez P, White P R, Alonso J B et al. Application of Teager-Kaiser energy operator to the analysis of degradation of a helicopter input pinion. The International Conference Surveillance 6, 2011.
15. Hryniewicz O. Theoretical advances and applications of fuzzy logic and soft computing. Advances in soft computing. In O. C, P. M, O.M. R et al. (eds): Theoretical Advances and Applications of Fuzzy Logic and Soft Computing, Berlin, Heidelberg, Springer Berlin Heidelberg: 2007; 42: 573-582.
16. Ibn Shamsah S M, Sinha J K. Rotor unbalance estimation with reduced number of sensors. Machines 2016, https://doi.org/10.3390/machines4040019.
17. Kaiser J F F. On a simple algorithm to calculate the "energy" of a signal. International Conference on Acoustics, Speech, and Signal Processing, IEEE: 1990; 407(1): 381-384, https://doi.org/10.1109/ICASSP.1990.115702.
18. Knotek J, Novotný P, Maršálek O et al. The Influence of Rotor Unbalance on Turbocharger Rotor Dynamics. Journal of Middle European Construction and Design of Cars 2016; 13(3): 8-13, https://doi.org/10.1515/mecdc-2015-0010.
19. Kosmol J. An extended model of angular bearing - influence of fitting and pre-deformation. Eksploatacja i Niezawodnosc - Maintenance and Reliability 2019; 21(3): 493-500, https://doi.org/10.17531/ein.2019.3.16.
20. Kozłowski E, Mazurkiewicz D, Żabiński T et al. Assessment model of cutting tool condition for real-time supervision system. Eksploatacja i Niezawodnosc - Maintenance and Reliability 2019; 21(4): 679-685, https://doi.org/10.17531/ein.2019.4.18.
21. Pawlik P. Single-number statistical parameters in the assessment of the technical condition of machines operating under variable load. Eksploatacja i Niezawodnosc - Maintenance and Reliability 2019; 21(1): 164-169, https://doi.org/10.17531/ein.2019.1.19.
22. Plantegenet T, Arghir M, Jolly P. Experimental analysis of the thermal unbalance effect of a flexible rotor supported by a flexure pivot tilting pad bearing. Mechanical Systems and Signal Processing 2020; 145: 106953, https://doi.org/10.1016/j.ymssp.2020.106953.
23. Rumin R. Mathematical models of balancing rotors based on mathematical and physical relationships. Advances in Science and Technology 2011; 8(8): 226-232.
24. Rumin R, Blaut J, Cieślik J. Application of Hurst exponent to the analysis of the rotor balancing device. Polish Congress of Mechanics, International conference on Computer Methods in Mechanics 2019.
25. Singh A, Gupta T C. Effect of rotating unbalance and engine excitations on the nonlinear dynamic response of turbocharger flexible rotor system supported on floating ring bearings. Archive of Applied Mechanics 2020, https://doi.org/10.1007/s00419-020-01660-z.
26. Spagnol J P, Wu H, Xiao K. Dynamic response of a cracked rotor with an unbalanced influenced breathing mechanism. Journal of Mechanical Science and Technology 2018; 32(1): 57-68, https://doi.org/10.1007/s12206-017-1207-9.
27. Wang A, Yao W, He K et al. Analytical modelling and numerical experiment for simultaneous identification of unbalance and rolling-bearing

coefficients of the continuous single-disc and single-span rotor-bearing system with Rayleigh beam model. Mechanical Systems and Signal Processing 2019; 116: 322-346, https://doi.org/10.1016/j.ymssp.2018.06.039.
28. Zhang C, Zhang Y. Common cause and load-sharing failures-based reliability analysis for parallel systems. Eksploatacja i Niezawodnosc - Maintenance and Reliability 2019; 22(1): 26-34, https://doi.org/10.17531/ein.2020.1.4.
29. Zhao B, Yuan Q, Li P. Improvement of the vibration performance of rod-fastened rotor by multioptimization on the distribution of original bending and unbalance. Journal of Mechanical Science and Technology 2020; 34(1): 83-95, https://doi.org/10.1007/s12206-019-1207-z.
30. Zou D, Zhao H, Liu G et al. Application of augmented Kalman filter to identify unbalance load of rotor-bearing system: Theory and experiment. Journal of Sound and Vibration 2019, https://doi.org/10.1016/j.jsv.2019.114972.
31. ISO 1940-1 Mechanical vibration - balance quality requirements for rotors in a constant (rigid) state. Part 1: Specification and verification of balance tolerances. 2003.
32. ISO 5343:1983 Criteria for evaluating flexible rotor balance. 1983.